International Journal of Automation and Computing 16(6), December 2019, 828-837
DOI: 10.1007/s11633-019-1182-y

Determination of Vertices and Edges in a Parametric Polytope to Analyze Root Indices of Robust Control Quality

Sergey Gayvoronskiy Tatiana Ezangina Ivan Khozhaev Viktor Kazmin

School of Computer Science and Robotics, National Research Tomsk Polytechnic University, Tomsk 634050, Russia

Abstract: The research deals with the methodology intended to root robust quality indices in the interval control system, the parameters of which are affinely included in the coefficients of a characteristic polynomial. To determine the root quality indices we propose to depict on the root plane not all edges of the interval parametric polytope (as the edge theorem says), but its particular vertex-edge route. In order to define this route we need to know the angle sequence at which the edge branches depart from any integrated pole on the allocation area. It is revealed that the edge branches can integrate into the route both fully or partially due to intersection with other branches. The conditions which determine the intersection of one-face edge images have been proven. It is shown that the root quality indices can be determined by its ends or by any other internal point depending on a type of edge branch. The conditions which allow determining the edge branch type have been identified. On the basis of these studies we developed the algorithm intended to construct a boundary vertex-edge route on the polytope with the interval parameters of the system. As an illustration of how the algorithm can be implemented, we determined and introduced the root indices reflecting the robust quality of the system used to stabilize the position of an underwater charging station for autonomous unmanned vehicles.

Keywords: Robust control, parametric uncertainty, parametric polytope, interval parameters, system analysis.

1 Introduction

Major challenge in modern industrial production is the development and design of high-quality automated control systems capable at operating when its parameters are unstable and not determined. In the real control systems the object parameters are often undetermined. It is connected with measuring errors, equipment ageing, and other disturbances impacting the object characteristics. Likewise, there are some systems, parameters of which can change in certain intervals. In both cases it is fair to apply the interval parameters approach to control systems synthesis. The systems, encompassing the control objects with interval parameters, are called interval control system (ICS)[1, 2]. Such systems can be introduced with the interval characteristic polynomials (ICP), the coefficients of which include the interval parameters of a control object. The character of how the interval parameters of ICS integrate into the ICP coefficients identifies a type of these coefficients uncertainty. There are four types of ICP coefficients uncertainty[1–3]: interval, affine, polylinear and polynomial.

The presence in ICS of non-stable parameters, which vary within certain intervals, can lead to a dynamic properties change in a system and result in its instability. The first research studies devoted to solving problems related to the analysis of ICS stability were performed by S. Dezoir, L. Zadeh and S. Faedo. The fundamental outcome in the field of ICS stability analysis with the focus on ICP coefficients was achieved by V. Kharitonov[4, 5]. Among the studies addressing the analysis of the robust stability are worth mentioning follows: J. Tsypkin, I. Vyshigorodsky, Yu. Neimark, B. Polyak, P. Shcherbakov, Yu. Petrov, J. Ackermann, B. R. Barmish, J. Kogan, R. Tempo, A. Packard, J. C. Doyle and others. In studies[6–21], the evaluation of ICP stability is performed within the frequency approach and probability approach. The studies based on μ-analysis are conducted in [22–25]. The studies based on Lyapunov functions are conducted in [26–28].

It is clear that ICS must be stable and support manipulated variables in allowable limits. Therefore, to date it stands more for the analysis of the robust quality than the analysis of the robust stability in ICS. In this field a root approach is the most illustrative one[29–38], when based on the allocation areas of ICP roots we can determine the requested indices of the robust quality – the degree of robust stability and the degree of robust oscillation. The simplest approach for it is the approach based on the edge theorem with the concept on a base of vertex-edge polynomials. A good development of this approach is performed in studies[36–40], where ICS is introduced with characteristic polynomials containing interval coefficients. These studies resulted in the methods according to which evaluation of the robust quality root indices

Research Article
Manuscript received November 11, 2018; accepted April 16, 2019; published online July 16, 2019
Recommended by Associate Editor James Whidborne

requires the analysis of only those vertices of coefficients polytope, which are depicted on the border of the allocation area of ICS poles.

It should be noted that the methods based on reduction of characteristic polynomial coefficients to an interval form (by rules of the interval analysis) leads to a conservative solution in case of ICS with the real interval parameters. Therefore, in order to increase the accuracy of ICS quality analysis it is necessary to consider the real interval physical parameters included in a certain way into the characteristic polynomial coefficients. Let us consider ICP, the coefficients of which integrate linearly into the physical parameters:

$$D(s) = \sum_{i=1}^{m} [T_i] A_i(s) + B(s) \tag{1}$$

where $[T_i] = [\underline{T}_i; \overline{T}_i]$. Such ICP are called polynomials with affine coefficients uncertainty. Example on how the ICP roots with affine coefficients uncertainty are projected on the complex plane is shown in Fig. 1.

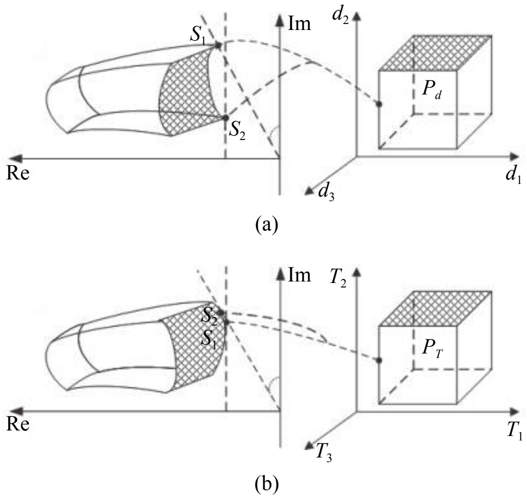

Fig. 1 Image of a parametric polytope with affine uncertainty of ICP coefficients. (a) Projections of a parametric polytope vertex on a complex plane; (b) Projection of an inner point of a parametric polytope edge on a complex plane.

As seen in Fig. 1, the required indices of ICS robust quality conform to the worst root indices when the interval parameters in prescribed limits are changed. In this case unlike the cases with the interval ICP coefficients uncertainty can be defined not only by the polytope vertices P_T (Fig. 1(a)), but also by the internal points of its edges (Fig. 1(b)). However, to depict all edges is a very complicated task. Considering the fact that the borders of the allocation area for ICP roots are not the images of all polytope edges P_T, but some of them, the interest is to determine the vertices and edges P_T, comprising a boundary vertex-edge route.

Hence, for ICS with affine ICP coefficients the task is set to develop the algorithm able to determine the robust stability and robust oscillability degree on the basis of boundary vertex-edge route.

2 Projection of an ICS parametric polytope on a root plane

ICP (1), whose coefficients include m interval parameters, form a rectangular hyper-parallelepiped $P_T = \{T_i \,|\underline{T_i} \le T_i \le \overline{T_i},\ i = \overline{1,m}\}$, with 2^m vertices and $m2^{m-1}$ edges. Let us define the vertices of P_T via V_q, $q = \overline{1, 2^m}$, where q is a number of vertices. Coordinates of every point of P_t edge in relation to a vertex V_q, $q = \overline{1, 2^m}$ can be determined with the following formula:

$$\begin{aligned} &T_i = T_i^q + \Delta T_i, \quad i = \overline{1,m} \\ &(\underline{T_i} - T_i^q) \le \Delta T_i \le (\overline{T_i} - T_i^q) \end{aligned} \tag{2}$$

where ΔT_i is the increment of i-th interval parameter, T_i^q is its value in vertex V_q. Based on introduced indices, we define the edge P_T via R_i^q. Each edge of P_T is reflected on the complex root plane (Fig. 2) on the basis of the equation

$$D^q(s) + \Delta T_i A_i(s) = 0 \tag{3}$$

where $D^q(s) = \sum_{i=1}^{m} T_i^q \cdot A_i(s) + B(s)$ is the vertex characteristic polynomial.

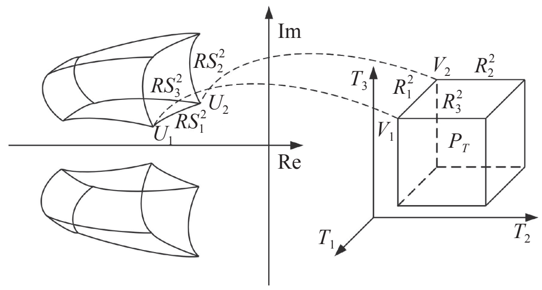

Fig. 2 Parametric polytope edges

If ICS with characteristic polynomial (3) has unity feedback, then its open-loop transfer function can be presented as

$$W_i^q(\Delta T_i, s) = \frac{\Delta T_i A_i(s)}{D^q(s)}. \tag{4}$$

Whereupon the root locus theory, when ΔT_i changes within the interval (2) the roots (3) form one-parameter interval root locus, the branches of which are called edge branches (RS_i^q), their starts and ends – a root node (U_q). Herewith, the expressions are correct: $\phi(R_i^q) = RS_i^q$, $\phi(V_q) = U_q$.

It is obvious that if two interval parameters T_i and T_j are changed, then, from one vertex V_q a rectangular face P_T is formed, which can be depicted through G_{ij}, and its image as GS_{ij} (Fig. 3).

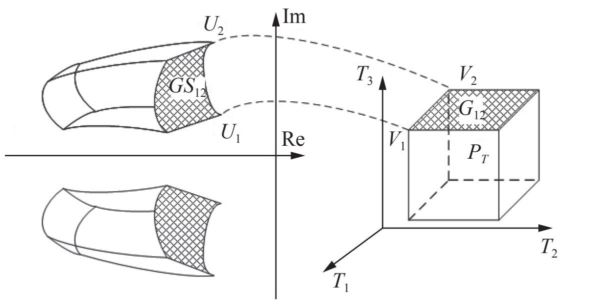

Fig. 3 Parametric polytope faces

When each ICS interval parameter is changed along the edge of any boundary vertex, the polynomial roots start moving along the edge branch, which departs from a vertex image at a corresponding angle. Let us define this angle as Θ_i^q. Based on the root locus theory, at increasing of T_i the angle Θ_i^q can be calculated with the formula $\Theta_i^q = 180° - \sum_{pol=1}^{n} \Theta_{pol} + \sum_{ze=1}^{vz} \Theta_{ze}$, at decreasing of T_i, we use the formula $\Theta_i^q = -\sum_{pol=1}^{n} \Theta_{pol} + \sum_{ze=1}^{vz} \Theta_{ze}$, where $\{\Theta_{pol}$ и $\Theta_{ze}\}$ is angles defined by the vectors coming from U_q corresponding to *pol*-th pole and to *ze*-th zero of transfer function (4). It should be noted that the value $\sum_{pol=1}^{n} \Theta_{pol}$ for all T_i is equal, therefore to determine the sequence of edge branches departure angles with T_i value, $\sum_{pol=1}^{n} \Theta_{pol}$ can be neglected. In case of increasing T_i, we will get

$$\Theta_i^q = 180° + \sum_{ze=1}^{vz} \Theta_{ze} \tag{5}$$

by decreasing T_i, we get

$$\Theta_i^q = \sum_{ze=1}^{vz} \Theta_{ze}. \tag{6}$$

Depending on the values found for the departure angles Θ_i^q, there can be constructed the sequence of how T_i parameters are changed from boundary root node. The example on roots departure at changing parameters T_i, $i = 1, 2, 3$ from the vertex V_q is shown in Fig. 4.

Due to the fact that the node U_q will be boundary node GU_q, it is needed that the root motion vectors with minimum Θ_1^{Vq} and maximum Θ_m^{Vq} departure angles will form the boundary angle, lying in a range [0°, 180°]. Introduce this statement on the basis of edge branches departure angles that have been calculated from a positive semiaxis

$$\left|\Theta_m^{Vq} - \Theta_1^{Vq}\right| < 180°. \tag{7}$$

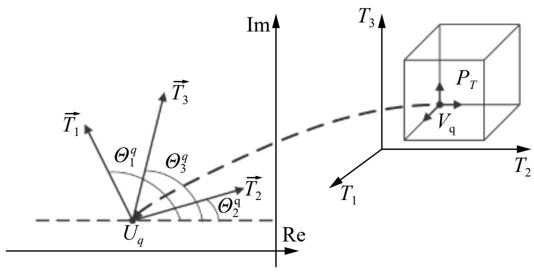

Fig. 4 Root motion direction at changing parameters from vertex of P_T

In so doing, a condition (7) allows defining the vertex P_T, the image of which belongs to an allocation area border S_r of a complex root.

3 Probability analysis on edge branches intersection belonging to one face

Suppose the prototypes RS_i и RS_j are the edges of one face. Consider the angles RS_i and RS_j departing from the root nodes of one boundary edge branch as GRS_k. If the sequence of these departure angles at the ends of the edge branch is of the same value, then, RS_i^q and RS_j^q will not intersect (Fig. 5). If for all faces of P_T with the common vertex, the same condition is fulfilled, then, the borders of the allocation area of a complex root are determined by non-intersected edge images of P_T.

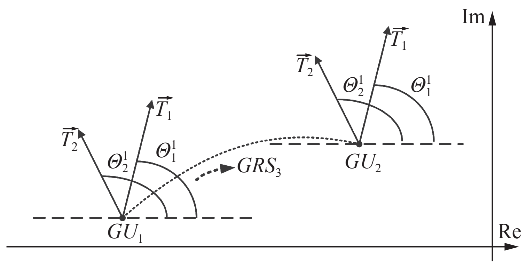

Fig. 5 A case of non-intersecting edge branches along T_1 and T_2

If at the ends of the boundary edge branch the sequence of departure angles RS_i^q and RS_j^q is not kept (Fig. 6), then, RS_i^q and RS_j^q are not intersected.

In this case the border of the allocation area of a complex root will consist of edge branches parts, which will be determined by the intersection points (Fig. 7).

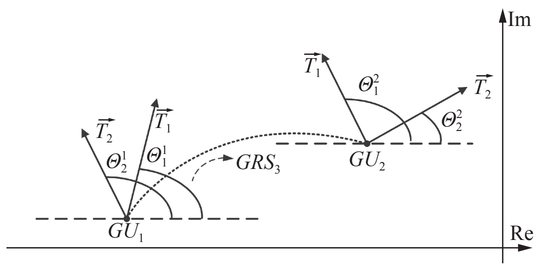

Fig. 6 A case of intersecting edge branches along T_1 and T_2

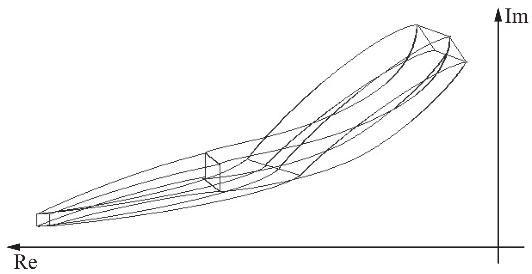

Fig. 7 Image of a parametric polytope when edge branches intersect

Let us define the conditions of edge branches intersection. Write down the equation reflecting face plane G_{ij}:

$$T_iA_i(s) + T_jA_j(s) + \sum_k T_k^qA_k(s) + B(s) = 0. \tag{8}$$

If in (8) we pose $s = s_r = \alpha + \mathrm{j}\beta$, $r \in \overline{1,n}$ and derive real and imaginary components, we will get the system of two linear equations, which connects s_r with two variables T_i and T_j

$$\begin{cases} T_i\mathrm{Re}A_i(\alpha,\beta) + T_j\mathrm{Re}A_j(\alpha,\beta) + \\ \qquad \mathrm{Re}\left[\sum\limits_k T_k^qA_k(s) + B(s)\right] = 0 \\ T_i\mathrm{Im}A_i(\alpha,\beta) + T_j\mathrm{Im}A_j(\alpha,\beta) + \\ \qquad \mathrm{Im}\left[\sum\limits_k T_k^qA_k(s) + B(s)\right] = 0. \end{cases} \tag{9}$$

Solving the system (9), two cases can be obtained:

1) The system has the single solution $T_i = T_i^*$, $T_j = T_j^*$. Then, $\phi^{-1}(s_r) = P^*$, $P^* = (T_i^*, T_j^*)$ and, consequently, the point $P^* \in G_{ij}^q$.

2) The equations are dependent and differ with a constant multiplier. In this case on the plane G_{ij}, there is a straight line h $(\phi^{-1}(s_r) = h)$, defined by any equation from the system (9).

Let us determine the composition of border area S_r of a complex root allocation, if $\varphi^{-1}(S_r) = G_{ij}$. It is clear that the coordinates P^* is the single possible solution (9), then, RS_i^q is the single branch coming through s_r. In this case the borders S_r consist of non-intersected edge images G_{ij}. If a prototype of root s_r is the straight line h, which is in the edge G_{ij} marks the interval $\overline{P_1P_2}$ (points P_1 and P_2 belong to the edges G_{ij}), then, through s_r (we call it the intersection node U^*) many root locus branches go along T_i and T_j, which lie between two intersected edge branches in s_r. In this case the borders S_r will consist of intersected edge images G_{ij}.

It is obvious that the required condition for the intersection node $U^* \in S_r$ is the straight line h, at least in one from the planes P_T, which have a common vertex. In order to find the equation linear relationship (9), testifying about the straight line h in the parameters' space T_i and T_j and its reflection in $U^*(\alpha, \mathrm{j}\beta)$, it is needed to verify the equation.

$$\frac{\mathrm{Re}A_i(\alpha,\beta)}{\mathrm{Im}A_i(\alpha,\beta)} = \frac{\mathrm{Re}A_j(\alpha,\beta)}{\mathrm{Im}A_j(\alpha,\beta)} = \frac{\mathrm{Re}\left[\sum\limits_k T_k^qA_k(\alpha,\beta) + B(\alpha,\beta)\right]}{\mathrm{Im}\left[\sum\limits_k T_k^qA_k(\alpha,\beta) + B(\alpha,\beta)\right]} \tag{10}$$

from (10) we obtain the following equation system:

$$\begin{cases} \mathrm{Re}A_i(\alpha,\beta)\,\mathrm{Im}A_j(\alpha,\beta) - \mathrm{Re}A_j(\alpha,\beta)\,\mathrm{Im}A_i(\alpha,\beta) = 0 \\ \mathrm{Re}A_j(\alpha,\beta)\,\mathrm{Im}\left[\sum\limits_k T_k^qA_k(\alpha,\beta) + B(\alpha,\beta)\right] - \\ \qquad \mathrm{Im}A_j(\alpha,\beta)\,\mathrm{Re}\left[\sum\limits_k T_k^qA_k(\alpha,\beta) + B(\alpha,\beta)\right] = 0. \end{cases} \tag{11}$$

If the system (11) does not have a solution when $\beta \neq 0$ for all interval parameters combinations, then, in S_r there is no U^* and the borders of S_r consist of non-intersected edge branches.

Suppose $A_i(s) = \sum_{w=0}^{z} a_{wi}s^w$, $A_j(s) = \sum_{c=0}^{l} a_{cj}s^w$. It has been defined if the degree z and l of polynomials $A_i(s)$ and $A_j(s)$ at interval parameters T_i and T_j are not higher than the second order, then, the analysis geared at the possibilities for edge branches intersection RS_i^q and RS_j^q does not require to solve the system (11), rather to check the condition fulfillment, which has been pointed out within the following statements.

Statement 1. If $A_i(s)$ and $A_j(s)$ are the first order, then, there is no edge images intersection for face G_{ij}.

Proof. The edge images intersections for face G_{ij} are possible, if (10) are dependent. Based on Moivre formula, we write down the first equation (10) in trigonometric form

$$\frac{\sum\limits_{w=0}^{z} a_{wi}|s|^w\cos(w\varphi)}{\sum\limits_{w=0}^{z} a_{wi}|s|^w\sin(w\varphi)} = \frac{\sum\limits_{c=0}^{l} a_{cj}|s|^c\cos(c\varphi)}{\sum\limits_{c=0}^{l} a_{cj}|s|^c\sin(c\varphi)}.$$

The equation from this equality is

$$\sum_{w=0}^{z} a_{wi}|s|^w\cos(w\varphi)\sum_{c=0}^{l} a_{cj}|s|^c\sin(c\varphi) = \sum_{w=0}^{z} a_{wi}|s|^w\sin(w\varphi)\sum_{c=0}^{l} a_{cj}|s|^c\cos(c\varphi).$$

On the base of which the other equation can be made

$$\sum_{w=0,c=0}^{z,l} a_{wi}a_{cj}|s|^{w+c}\sin\left((c-w)\varphi\right)=0,\ w\neq c. \quad (12)$$

Suppose $z=1$; $l=1$, then $a_{0i}a_{1j}|s|^{1}\sin(\varphi)-a_{1i}a_{0j}\times|s|^{1}\sin(\varphi)=0$. Thus, $\sin(\varphi)\neq 0$, then, in solving this equation, we will obtain $a_{0i}a_{1j}=a_{1i}a_{0j}$. The result says that when T_i and T_j are changed, the edge branches RS_i^q and RS_j^q depart from the vertex image at the same angle and coincide with each other. □

Statement 2. If $A_i(s)$ and $A_j(s)$ are the second order, then, there is no edge images intersections for face G_{ij} in case when the inequations are fulfilled for all pairs of the interval parameters as T_i and T_j

$$\begin{aligned}&(a_{1i}a_{2j}-a_{2i}a_{1j})(a_{0i}a_{1j}-a_{1i}a_{0j})\geq(a_{0i}a_{2j}-a_{2i}a_{0j})^2\\&a_{1i}a_{2j}-a_{2i}a_{1j}\leq 0\\&4(a_{0i}a_{1j}-a_{1i}a_{0j})(a_{1i}a_{2j}-a_{2i}a_{1j})\geq 0.\end{aligned} \quad (13)$$

Proof. Suppose $z=2$; $l=2$. Then, based on (12) let us write down

$$a_{0i}a_{1j}|s|^{1}\sin(\varphi)-a_{1i}a_{0j}|s|^{1}\sin(\varphi)+a_{0i}a_{2j}|s|^{2}\sin(2\varphi)-a_{2i}a_{0j}|s|^{2}\sin(2\varphi)+a_{1i}a_{2j}|s|^{3}\sin(\varphi)-a_{2i}a_{1j}|s|^{3}\sin(\varphi)=0.$$

After the equation rearrangement, we obtain $\sin(\varphi)\times(a_{0i}a_{1j}-a_{1i}a_{0j}+a_{1i}a_{2j}|s|^{2}-a_{2i}a_{1j}|s|^{2})+2\sin(\varphi)\cos(\varphi)\times(a_{0i}a_{2j}|s|^{1}-a_{2i}a_{0j}|s|^{1})=0$.

The solution $|s|$ (see the equation at the bottom) for this equation will be real and positive.

If the following conditions are fulfilled.

1) $a_{1i}a_{2j}-a_{2i}a_{1j}>0$.

2) $4\cos^2(\varphi)(a_{0i}a_{2j}-a_{2i}a_{0j})^2-4(a_{0i}a_{1j}-a_{1i}a_{0j})\times(a_{1i}a_{2j}-a_{2i}a_{1j})>0$, consequently, $\cos^2(\varphi)>\dfrac{(a_{0i}a_{1j}-a_{1i}a_{0j})(a_{1i}a_{2j}-a_{2i}a_{1j})}{(a_{0i}a_{2j}-a_{2i}a_{0j})^2}$. Thus, $\cos^2(\varphi)<1$, then, $\dfrac{(a_{0i}a_{1j}-a_{1i}a_{0j})(a_{1i}a_{2j}-a_{2i}a_{1j})}{(a_{0i}a_{2j}-a_{2i}a_{0j})^2}<1$. Hence, the second condition $(a_{0i}a_{1j}-a_{1i}a_{0j})(a_{1i}a_{2j}-a_{2i}a_{1j})<(a_{0i}a_{2j}-a_{2i}a_{0j})^2$.

3) $2\cos(\varphi)(a_{2i}a_{0j}-a_{0i}a_{2j})-\sqrt{4\cos^2(\varphi)(a_{0i}a_{2j}-a_{2i}a_{0j})^2-4(a_{0i}a_{1j}-a_{1i}a_{0j})(a_{1i}a_{2j})\times}\sqrt{-a_{2i}a_{1j})}>0$, hence, after the rearrangement it follows that $2\cos^2(\varphi)(a_{0i}a_{2j}-a_{2i}a_{0j})>(a_{0i}a_{1j}-a_{1i}a_{0j})\times(a_{1i}a_{2j}-a_{2i}a_{1j})$.

Then, $\cos^2(\varphi)>\dfrac{(a_{0i}a_{1j}-a_{1i}a_{0j})(a_{1i}a_{2j}-a_{2i}a_{1j})}{2(a_{0i}a_{2j}-a_{2i}a_{0j})^2}$, and, hence, $\dfrac{(a_{0i}a_{1j}-a_{1i}a_{0j})(a_{1i}a_{2j}-a_{2i}a_{1j})}{2(a_{0i}a_{2j}-a_{2i}a_{0j})^2}<1$. In so doing, the third condition is $(a_{0i}a_{1j}-a_{1i}a_{0j})(a_{1i}a_{2j}-a_{2i}a_{1j})<2(a_{0i}a_{2j}-a_{2i}a_{0j})^2$.

4) $2\cos(\varphi)(a_{2i}a_{0j}-a_{0i}a_{2j})+\sqrt{4cos^2(\varphi)(a_{0i}a_{2j}-a_{2i}a_{0j})^2-4(a_{0i}a_{1j}-a_{1i}a_{0j})(a_{1i}a_{2j}-a_{2i}a_{1j})}>0$.

Then, the fourth condition is $4(a_{0i}a_{1j}-a_{1i}a_{0j})(a_{1i}a_{2j}-a_{2i}a_{1j})<0$. □

Statement 2 leads to two conclusions.

Conclusion 1. If $z=1$, $l=2$, then, there is no edge images intersections in face G_{ij} in case when the inequations are fulfilled for all pairs of the interval parameters as T_i and T_j

$$\begin{aligned}&a_{1i}a_{2j}(a_{0i}a_{1j}-a_{1i}a_{0j})\geq(a_{0i}a_{2j})^2\\&4a_{1i}a_{2j}(a_{0i}a_{1j}-a_{1i}a_{0j})\geq 0.\end{aligned} \quad (14)$$

Conclusion 2. If $z=2$, $l=1$, then, there is no edge images intersections in face G_{ij} in case when the inequalities are fulfilled for all pairs of the interval parameters as T_i and T_j

$$\begin{aligned}&a_{2i}a_{1j}(a_{1i}a_{0j}-a_{0i}a_{1j})\geq(a_{2i}a_{0j})^2\\&4a_{2i}a_{1j}(a_{1i}a_{0j}-a_{0i}a_{1j})\geq 0.\end{aligned} \quad (15)$$

Consequently, the methodology on the possibility analysis geared at edge images intersection for face G_{ij} consists of the following stages.

1) Write down ICP as (1).

2) If the degree of all polynomials at interval parameters is not higher than the second order, then, it is necessary to check if the conditions (13)–(15) are properly fulfilled.

3) If the conditions (13)–(15) are not fulfilled, then, there is edge images intersections for face G_{ij}.

4) If among polynomials at interval parameters, there are polynomials of the third order and higher, then, it is necessary to choose an optional vertex V_q, $q\in\overline{1,2^m}$ and to solve the equation system for all faces concurrent in it (11).

4 Analysis of edge branches types

If the edge branch point, which is the nearest one to an imaginary axis, is one of the edge ends as shown in Fig. 8 (a), then, this edge branch can be classified as the first type. If the nearest to an imaginary axis is one of the inner roots of the edge branch, it is referred to the second type (Fig. 8 (b)). The types of boundary edge branches are important to know when defining the root quality indices. For example, if the branch is of the first type, then, in order to define the minimal degree of stability and the maximum degree of oscillability, there is no need to build this edge branch, but it is enough to define the roots at the edge ends.

$$|s|=\frac{2\cos(\varphi)(a_{2i}a_{0j}-a_{0i}a_{2j})\pm\sqrt{4\cos^2(\varphi)(a_{0i}a_{2j}-a_{2i}a_{0j})^2-4(a_{0i}a_{1j}-a_{1i}a_{0j})(a_{1i}a_{2j}-a_{2i}a_{1j})}}{2(a_{1i}a_{2j}-a_{2i}a_{1j})}.$$

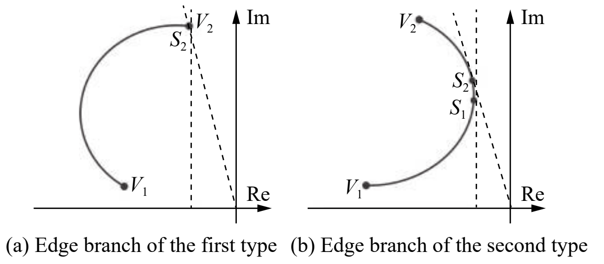

(a) Edge branch of the first type (b) Edge branch of the second type

Fig. 8 Edge branches of parametric polytope

Condition 1. If polynomials $A_i(s)$ at interval parameters T_i are the polynomials of the first degree or of even and odd degree s, as well as a product of two polynomials, then, the edge branch RS_i^q is the branch of the first type. For other polynomials $A_i(s)$, the following condition is valid.

Condition 2. If the condition is fulfilled as

$$\frac{\partial \arg((\overline{\mathrm{T}_i}-\underline{\mathrm{T}_i})\mathrm{A}_i(\mathrm{j}\beta))}{\partial\beta}\le\left|\frac{\sin(2\arg((\overline{\mathrm{T}_i}-\underline{\mathrm{T}_i})\mathrm{A}_i(\mathrm{j}\beta)))}{2\beta}\right| \quad (16)$$

then, the edge branch RS_i^q can be the first-type one.

Consequently, when these conditions are used, we can define the type for all edge branches arriving into the boundary route.

5 Methodology used to determine the root indices of ICS robust quality

Considered research resulted in the methodology, based on constructing a vertex-edge route, applicable to determine the root indices of ICS robust quality. The methodology includes the following stages:

1) Deriving an ICP (1).

2) Defining the coordinates of polytope P_T vertices.

3) Calculating a polynomial complex root U_q for the arbitrary V_q, $q\in\overline{1,2^m}$.

4) Finding m angles Θ_i^q, $i\in\overline{1,m}$ for U_q based on (5) and (6).

5) Verification of inhering U_q to the border S_r based on (7). If at least one condition (7) is not fulfilled, it should be chosen the other vertex P_T and repeat the attempt, points from 3) to 5) above.

6) For the value found GU_q the consequence of departure angles based on the interval parameters T_i for edge branches should be composed.

7) Based on the consequence Θ_i^q, $i\in\overline{1,m}$ the direct edge route can be built, which will depart from GU_q and include $2m$ of edges.

8) Defining faces G_{ij}, edge images RS_i^q, which can intersect.

9) If two consequent edges R_i^q and R_j^q of the edge route are the edges of face G_{ij} and their images can intersect, then, two opposite edges of this face should be added to the direct edge route.

10) If while constructing the route we get repeated edges, they should be united.

11) Defining the type of edge branches entering the constructed edge route.

12) If the edge branch RS_i^q is referred to the first type, then, it is deleted from the edge route. If the edge branches of the first type are connected consequently, then, in the route only vertices connecting them are left.

13) Introducing a boundary vertex-edge route to the root plane and defining the root indices of ICS robust quality (a degree of robust oscillability and stability) according to allocation areas of ICP roots.

6 Numerical illustration

Let us consider a system responsible for automated position stabilization in a charging station to be merged with a tether for autonomous unmanned underwater vehicles. The structural scheme is described in Fig. 9.

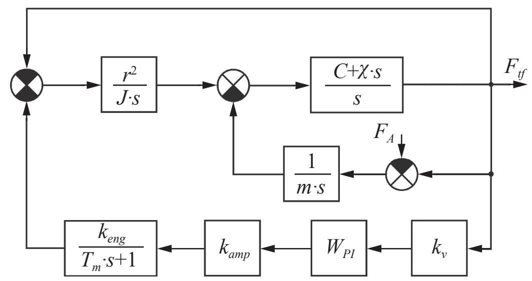

Fig. 9 System structural diagram

In Fig. 9, k_{eng} is the voltage transfer coefficient of an engine; k_{amp} is transfer coefficient of an amplifying device; $C=\dfrac{C_1}{l}$ is tether hardness coefficient, $C_1=10^5$ N is specific tether hardness coefficient; $\chi=\dfrac{\chi_1}{l}$ is the relative loss coefficient for tether elasticity, $\chi_1=10^4$ N·s is specific coefficient of tether elasticity loss; $r=0.1$ m is hoist drum radius; $k_1=1-$transfer coefficient of PI-controller, $k_2=0.01$ is time constant for PI-controller, $m=[50;\,500]$ kg is charging station mass and underwater vehicle mass; $l=[50;\,100]$ m is tether length; $k=k_{amp}\cdot k_{eng}\cdot k_v=[5;\,15]$ is transfer coefficient of electric drive.

As a result of structural transformations we obtain the interval characteristic polynomial:

$$D(s)=[d_4]s^4+[d_3]\cdot s^3+[d_2]\cdot s^2+[d_1]\cdot s+[d_0] \quad (17)$$

where $[d_0]=[m]\,C_{y\partial}\,[k]\,k_1r^2$; $[d_1]=(C_{y\partial}(J+[m]r^2(1+k_2[k]))+\chi_{y\partial}[m]r^2k_1k)$; $[d_2]=(T_mC_{y\partial}(r^2[m]+J)+\chi_{y\partial}(J+[m]r^2(1+k_2k)))$; $[d_3]=(J[l][m]+T_m\chi_{y\partial}(r^2[m]+J)$; $[d_4]=J[l][m]T_m$.

The interval parameters $[m]$, $[l]$, $[k]$ are linearly included into ICP coefficients (17) (set the affine coefficients uncertainty) and are formed interval parametric polytope P_T. The polytope P_T possesses 8 vertices: $V_1(\underline{m}, \underline{l}, \underline{k})$, $V_2(\underline{m_1}, \overline{l}, \underline{k})$, $V_3(\underline{m}, \overline{l}, \overline{k})$, $V_4(\overline{m}, \underline{l}, \underline{k})$, $V_5(\overline{m}, \overline{l}, \underline{k})$, $V_6(\overline{m}, \overline{l}, \overline{k})$, $V_7(\overline{m}, \underline{l}, \overline{k})$,$V_8(\underline{m}, \underline{l}, \overline{k})$. Then, ICP (1) with the affine coefficients uncertainty looks as

$$[T_1] \cdot A_1(s) + \frac{1}{[T_2]} \cdot A_2(s) + [T_3] \cdot A_3(s) + B(s) = 0 \quad (18)$$

where $[T_1] = [l]$; $[T_2] = [m]$; $[T_3] = [k]$; $A_1(s) = Js^3(T_m s + 1)$; $A_2(s) = Js((T_m s + 1)(\chi_1 s + C_1))$; $A_3(s) = r^2((\chi_1 s + C_1)(k_2 s + k_1))$; $B(s) = r^2 s((\chi_1 s + C_1)(T_m s + 1))$. It is necessary to determine the vertices and edges of the polytope P_T, which will help to define the root indices of the robust quality in a system able to stabilize a position of a charging station to be merged.

According to the algorithm, the polynomial roots in the first vertex have been defined in (18) [–10; –31.3; –6.3 – j4.88; –6.3 + j4.88], and the roots of polynomial $A_1(s)$ as well: [0; 0; 0; –10], $A_2(s)$: [0; 0; –10], $A_3(s)$: [–100; –10]. Further, for the image of the first vertex $U_1 = -6.3 + $ j4.88 based on (5) and (6) the departure angles of the edge branches have been calculated with the following interval parameters: $\Theta_{T_1}^{V1} = 146.34°$, $\Theta_{T_2}^{V1} = 93.94°$, $\Theta_{T_3}^{V1} = 82°$. As long as the condition (7) is fulfilled, then, U_1 is a boundary vertex and belongs to the edge route. By virtue of the fact that $\Theta_{T_3}^{V1} < \Theta_{T_2}^{V1} < \Theta_{T_1}^{V1}$, then, in the edge route the interval parameters depart from the vertex V_1 in the following consequence: $T_3 \to T_2 \to T_1 \to T_3 \to T_2 \to T_1$. This consequence accords with the direct edge route as shown in Fig. 10.

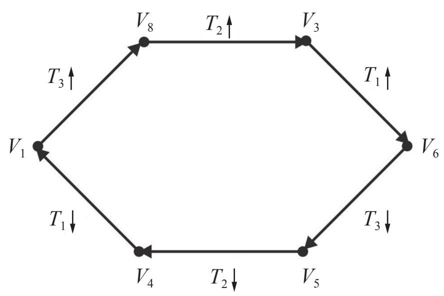

Fig. 10 Direct edge route

Let us verify if boundary edge route has intersected edge branches. In the vertex V_1 three faces G_{32}, G_{21}, G_{31} meet, where the indices comply with the indices of the interval parameters. Given that the polynomials $A_1(s)$, $A_2(s)$ have a higher than the second degree, then, for faces G_{32}, G_{21}, G_{31} three equation systems can be composed in (11). Having solved these equations, we obtain two roots: $s_{1,2} = -5.55 \pm$ j8.96, corresponding to the coordinates of a possible intersection for the edge images of faces G_{32}, G_{21}, G_{31}. In so doing, boundary edge route will be viewed as shown in Fig. 11.

As a final stage let us define the type of edge branches in the edge route to be constructed. For the polynomial

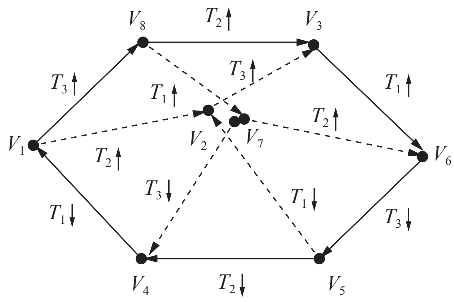

Fig. 11 Edge route

$A_1(s)$ the condition 1 is fulfilled, hence, the branches along T_1 have the first type. However, this condition does not cover the polynomials $A_2(s)$ and $A_3(s)$. Therefore, in order to define a branch type along T_2 and T_3 we need to verify the condition (16) and we will get

$$\frac{\partial \arg\left(\left(\frac{1}{\underline{T_2}} - \frac{1}{\overline{T_2}}\right) A_2(\mathrm{j}\beta)\right)}{\partial \beta} > \left| \frac{\sin\left(2 \arg\left(\left(\frac{1}{\underline{T_2}} - \frac{1}{\overline{T_2}}\right) A_2(\mathrm{j}\beta)\right)\right)}{2\beta} \right|,$$

$$\frac{\partial \arg\left(\left(\overline{T_3} - \underline{T_3}\right) A_3(\mathrm{j}\beta)\right)}{\partial \beta} > \left| \frac{\sin(2 \arg((\overline{T_3} - \underline{T_3}) A_3(\mathrm{j}\beta)))}{2\beta} \right|,$$ it shows that the edge branches along T_2 and T_3 are the second type ones. Consequently, the vertex-edge route has the view as seen in Fig. 12.

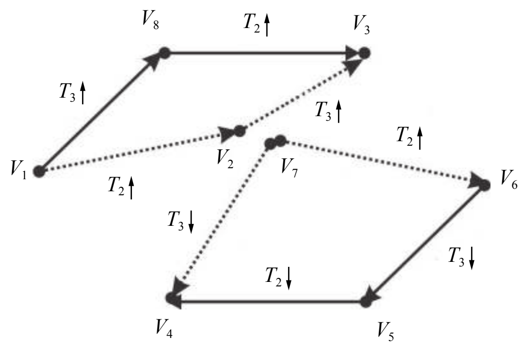

Fig. 12 Boundary vertex-edge route

With the aim of defining the root quality indices we put the route on the root plane (Fig. 13). As seen in Fig. 13, the degree of the robust system stability responsible for the stabilization of the charging station at merging is $\alpha = 1.62$, the degree of its robust oscillability is $\mu = 8.13$; it corresponds to a sector with the angle $\varphi = \pm 82°$. These quality indices are defined by a vertex image. $V_6(\overline{T_1}; \overline{T_2}; \overline{T_3})$. It should be noted that sufficiently high oscillability in a merged station position stabilization can be explained by tether elasticity properties in combination with a low coefficient of damping effect.

Fig. 14 presents transient processes in two vertices of a boundary route, one of them corresponds to a minimum oscillability degree of the system stability ($V6$), the second one - to maximal value of oscillability degree ($V4$).

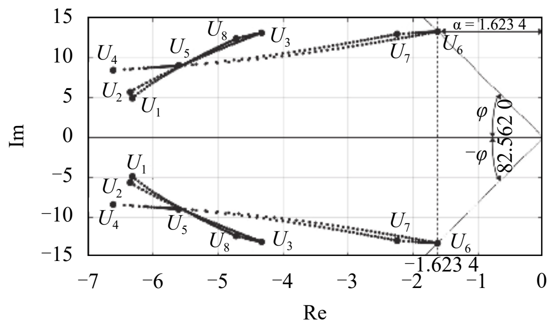

Fig. 13 Vertexes and edges in boundary route

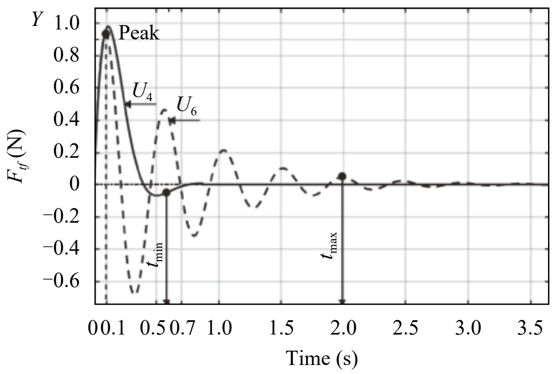

Fig. 14 Vertexes and edges in boundary route

As seen in Fig. 14, the minimum constant time is $t_{\max} = 0.58$ (in $V_4(\overline{T_1};\ \underline{T_2};\ \underline{T_3})$), and the maximum constant time is $t_{\max} = 1.98$ (in $V_6(\overline{T_1};\ \overline{T_2};\ \overline{T_3})$). The latter index corresponds to the found degree of the robust stability α that proves the correctness in evaluation of the system quality root indices.

7 Discussions

The research gives the ground to conclude that when using the interval and affine uncertainty of ICP, the more accurate root allocation area is obtained with affine uncertainty. It is located inside the area constructed after reducing ICP coefficients to the interval view. It states that in transmitting from the interval parameters towards the interval coefficients as ICP, the control quality indices can be significantly decreased. Let us reaffirm this conclusion with the comparison of the robust quality analysis accuracy of the system studied above, when ICP has the affine uncertainty of the coefficients. For the second case, in Fig. 15, we introduced the polynomial vertices of ICP coefficients obtained through construction of the vertex route.

The figure illustrates that the system, which is relatively stable at affine uncertainty of ICP coefficients, and is responsible for charging station position stabilization in merging process, turned out to be non-stable after the coefficients have been reduced to the interval view.

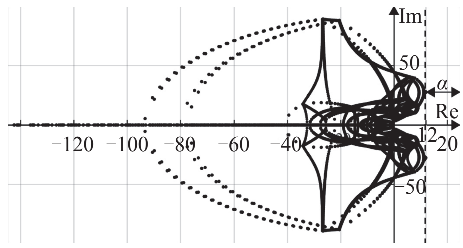

Fig. 15 Vertexes of boundary route

8 Conclusions

For ICS with affine uncertainty of ICP coefficients the following properties of boundary vertex-edge route of a parametric polynomial have been set:

1) The route can be composed of non-intersected edge branches RS_i^q in the ordering corresponding to the departure angles sequence RS_i^q from any boundary pole;

2) The route can include intersecting edge branches RS_i^q and RS_j^q, which can be defined via the algebraic conditions in the view of the proven statements;

3) The first type edge branches can be deleted from the route, having left only their boundary root nodes.

On the basis of the properties presented above, we developed the algorithm enabling to construct a boundary vertex-edge polytope with the interval system parameters. Its projection to the root plane defines the root robust quality indices of ICS.

It is shown that in transmitting from the interval system parameters towards the interval ICP coefficients the root allocation area of ICP is significantly enlarged. That results in reducing the robust quality indices of the system.

Acknowledgements

This work was supported by the Ministry of Education and Science of the Russian Federation (No. 2.3649. 2017/PCh).

References

[1] S. P. Bhattacharyya. Robust control under parametric uncertainty: An overview and recent results. *Annual Reviews in Control*, vol. 44, pp. 45–77, 2017. DOI: 10.1016/j.arcontrol.2017.05.001.

[2] J. Ackermann. *Robust Control: Systems with Uncertain Physical Parameters*, London, UK: Springer-Verlag, pp. 57–76, 1993.

[3] D. Mihailescu-Stoica, F. Schrodel, R. Vobetawinkel, J. Adamy. On robustly stabilizing PID controllers for systems with a certain class of multilinear parameter dependency. In *Proceedings of the 26th Mediterranean Conference on Control and Automation*, IEEE, Zadar, Croatia, pp. 1–6, 2018. DOI: 10.1109/MED.2018.8442811.

[4] Y. V. Hote. Necessary conditions for stability of Kharitonov polynomials. *IETE Technical Review*, vol. 28, no. 5,

pp. 445–448, 2011. DOI: 10.4103/0256-4602.85977.

[5] B. Y. Juang. Robustness of pole assignment of an interval polynomial using like λ-degree feedback gain based on the Kharitonov theorem. In *Proceedings of SICE Annual Conference*, IEEE, Taipei, China, pp. 3475–3484, 2010.

[6] A. Karimi, A. Nicoletti, Y. M. Zhu. Robust H_∞ controller design using frequency-domain data via convex optimization. *International Journal of Robust and Nonlinear Control*, vol. 28, no. 12, pp. 3766–3783, 2018. DOI: 10.1002/rnc.3594.

[7] T. A. Bryntseva, A. L. Fradkov. Frequency-domain estimates of the sampling interval in multirate nonlinear systems by time-delay approach. *International Journal of Control*, pp. 1–8, 2018. DOI: 10.1080/00207179.2017.1423394.

[8] Y. Hwang, Y. R. Ko, Y. Lee, T. H. Kim. Frequency-domain tuning of robust fixed-structure controllers via quantum-behaved particle swarm optimizer with cyclic neighborhood topology. *International Journal of Control, Automation and Systems*, vol. 16, no. 2, pp. 426–436, 2018. DOI: 10.1007/s12555-016-0766-3.

[9] B. Basu, A. Staino. Time-frequency control of linear time-varying systems using forward Riccati differential equation. In *Proceedings of Indian Control Conference*, IEEE, Kanpur, India, pp. 223–228, 2018. DOI: 10.1109/INDIANCC.2018.8307982.

[10] J. Garcia-Tirado, H. Botero, F. Angulo. A new approach to state estimation for uncertain linear systems in a moving horizon estimation setting. *International Journal of Automation and Computing*, vol. 13, no. 6, pp. 653–664, 2016. DOI: 10.1007/s11633-016-1015-1.

[11] A. Khalil, J. H. Wang, O. Mohamed. Robust stabilization of load frequency control system under networked environment. *International Journal of Automation and Computing*, vol. 14, no. 1, pp. 93–105, 2017. DOI: 10.1007/s11633-016-1041-z.

[12] Z. Gao, L. R. Zhai, Y. D. Liu. Robust stabilizing regions of fractional-order PI^λ controllers for fractional-order systems with time-delays. *International Journal of Automation and Computing*, vol. 14, no. 3, pp. 340–349, 2017. DOI: 10.1007/s11633-015-0941-7.

[13] M. S. Sunila, V. Sankaranarayanan, K. Sundareswaran. Comparative analysis of optimized output regulation of a SISO nonlinear system using different sliding manifolds. *International Journal of Automation and Computing*, vol. 14, no. 4, pp. 450–462, 2017. DOI: 10.1007/s11633-017-1078-7.

[14] Y. Jiang, J. Y. Dai. An adaptive regulation problem and its application. *International Journal of Automation and Computing*, vol. 14, no. 2, pp. 221–228, 2017. DOI: 10.1007/s11633-015-0900-3.

[15] A. Zouhri, I. Boumhidi. Decentralized robust H_∞ control of large scale systems with polytopic-type uncertainty. *International Review on Automatic Control*, vol. 9, no. 2, pp. 103–109, 2016. DOI: 10.15866/ireaco.v9i2.8728.

[16] M. Khadhraoui, M. Ezzine, H. Messaoud, M. Darouach. Full order H_∞ filter design for delayed singular systems with unknown input and bounded disturbance: Time and frequency domain approaches. *International Review on Automatic Control*, vol. 9, no. 1, pp. 26–39, 2016. DOI: 10.15866/ireaco.v9i1.7843.

[17] B. B. Alagoz, C. Yeroglu, B. Senol, A. Ates. Probabilistic robust stabilization of fractional order systems with interval uncertainty. *ISA Transactions*, vol. 57, pp. 101–110, 2015. DOI: 10.1016/j.isatra.2015.01.003.

[18] H. S. Ahn, Y. Q. Chen. Necessary and sufficient stability condition of fractional-order interval linear systems. *Automatica*, vol. 44, no. 11, pp. 2985–2988, 2008. DOI: 10.1016/j.automatica.2008.07.003.

[19] B. Senol, A. Ates, B. B. Alagoz, C. Yeroglu. A numerical investigation for robust stability of fractional-order uncertain systems. *ISA Transactions*, vol. 53, no. 2, pp. 189–198, 2014. DOI: 10.1016/j.isatra.2013.09.004.

[20] J. G. Lu, Y. Q. Chen. Robust stability and stabilization of fractional-order interval systems with the fractional order α: The $0 < \alpha < 1$ case. *IEEE Transactions on Automatic Control*, vol. 55, no. 1, pp. 152–158, 2010. DOI: 10.1109/TAC.2009.2033738.

[21] I. N'Doye, M. Darouach, M. Zasadzinski, N. E. Radhy. Robust stabilization of uncertain descriptor fractional-order systems. *Automatica*, vol. 49, no. 6, pp. 1907–1913, 2013. DOI: 10.1016/j.automatica.2013.02.066.

[22] P. M. Young, M. P. Newlin, J. C. Doyle. μ analysis with real parametric uncertainty. In *Proceedings of the 30th IEEE Conference on Decision and Control*, Brighton, UK, vol. 2, pp. 1251–1256, 1991. DOI: 10.1109/CDC.1991.261579.

[23] S. Sumsurooah, M. Odavic, S. Bozhko. μ approach to robust stability domains in the space of parametric uncertainties for a power system with ideal CPL. *IEEE Transactions on Power Electronics*, vol. 33, no. 1, pp. 833–844, 2018. DOI: 10.1109/TPEL.2017.2668900.

[24] S. Sumsurooah, M. Odavic, S. Bozhko, D. Boroyevic. Toward robust stability of aircraft electrical power systems: Using a μ-based structural singular value to analyze and ensure network stability. *IEEE Electrification Magazine*, vol. 5, no. 4, pp. 62–71, 2017. DOI: 10.1109/MELE.2017.2757383.

[25] K. Chaker, A. Moussaoui, B. Sbartai. μ-synthesis control applied to counter the seismic load action on a building structure. *International Review of Automatic Control*, vol. 10, no. 1, pp. 92–99, 2017. DOI: 10.15866/ireaco.v10i1.10617.

[26] B. K. Sahu, B. Subudhi, M. M. Gupta. Stability analysis of an underactuated autonomous underwater vehicle using extended-routh's stability method. *International Journal of Automation and Computing*, vol. 15, no. 3, pp. 299–309, 2018. DOI: 10.1007/s11633-016-0992-4.

[27] X. Q. Zhang, X. Y. Li, J. Zhao. Stability analysis and anti-windup design of switched systems with actuator saturation. *International Journal of Automation and Computing*, vol. 14, no. 5, pp. 615–625, 2017. DOI: 10.1007/s11633-015-0920-z.

[28] Z. Liu, Y. Z. Wang. Regional stability of positive switched linear systems with multi-equilibrium points. *International Journal of Automation and Computing*, vol. 14, no. 2, pp. 213–220, 2017. DOI: 10.1007/s11633-016-1003-5.

[29] F. D. C. Da Silva, J. B. De Oliveira, A. D. De Araujo. Robust interval adaptive pole-placement controller based on variable structure systems theory. In *Proceedings of the 25th International Conference on Systems Engineering*, IEEE, Las Vegas, USA, pp. 45–54, 2017. DOI: 10.1109/ICSEng.2017.73.

[30] W. Wiboonjaroen, T. Sooknuan, M. Thumma. Robust pole placement by state-Pi feedback control for interval plants. In *Proceedings of Computing Conference*, IEEE, London, UK, pp. 1350–1356, 2017. DOI: 10.1109/SAI.2017.8252266.

[31] L. H. Keel, S. P. Bhattacharyya. Robustness and fragility of high order controllers: A tutorial. In *Proceedings of IEEE Conference on Control Applications*, IEEE, Buenos Aires, Argentina, pp. 191–202, 2016. DOI: 10.1109/CCA.2016.7587837.

[32] A. A. Nesenchuk. A method for synthesis of robust interval polynomials using the extended root locus. In *Proceedings of American Control Conference*, IEEE, Seattle, USA, pp. 1715–1720, 2017. DOI: 10.23919/ACC.2017.7963200.

[33] Y. Chursin, D. Sonkin, M. Sukhodoev, R. Nurmuhametov, V. Pavlichev. Control system for an object with interval-given parameters: Quality analysis based on leading coefficients of characteristic polynomials. *International Review of Automatic Control*, vol. 11, no. 4, pp. 203–207, 2018. DOI: 10.15866/ireaco.v11i4.15727.

[34] B. Senol, C. Yeroglu. Robust stability analysis of fractional order uncertain polynomials. In *Proceedings of the 5th IFAC Workshop on Fractional Differentiation and its Applications*, Nanjing, China, pp. 1–6, 2012.

[35] A. V. Egorov, C. Cuvas, S. Mondie. Necessary and sufficient stability conditions for linear systems with pointwise and distributed delays. *Automatica*, vol. 80, pp. 218–224, 2017. DOI: 10.1016/j.automatica.2017.02.034.

[36] S. A. Gayvoronskiy, T. Ezangina. The algorithm of analysis of root quality indices of high order interval systems. In *Proceedings of the 27th Chinese Control and Decision Conference*, IEEE, Qingdao, China, pp. 3048–3052, 2015. DOI: 10.1109/CCDC.2015.7162444.

[37] O. S. Vadutov, S. A. Gayvoronskiy. Application of edge routing to the stability analysis of interval polynomials. *Izvestiya Akademii Nauk. Teoriya i Sistemy Upravleniya*, vol. 6, pp. 7–12, 2003.

[38] S. A. Gayvoronskiy, T. Ezangina, I. Khozhaev. The analysis of permissible quality indices of the system with affine uncertainty of characteristic polynomial coefficients. In *Proceedings of International Automatic Control Conference*, IEEE, Taichung, China, pp. 30–34, 2016. DOI: 10.1109/CACS.2016.7973879.

[39] B. B. Alagoz. A note on robust stability analysis of fractional order interval systems by minimum argument vertex and edge polynomials. *IEEE/CAA Journal of Automatica Sinica*, vol. 3, no. 4, pp. 411–421, 2016. DOI: 10.1109/JAS.2016.7510088.

[40] C. Othman, I. Ben Cheikh, D. Soudani. On the internal multi-model control of uncertain discrete-time systems. *International Journal of Advanced Computer Science and Applications*, vol. 7, no. 9, pp. 88–98, 2016. DOI: 10.14569/IJACSA.2016.070912.

Sergey Gayvoronskiy received the Ph. D. degree in control systems engineering from the Tomsk Polytechnic University, Russia in 1990. He is presently an associated professor of the Division for Automation and Robotics at the School of Computer Science and Robotics, National Research Tomsk Polytechnic University, Russia. He was repeatedly awarded by Ministry of Education and Science of Russian Federation, Russian Union of Young Scientists and Tomsk Polytechnic University for his educational and scientific achievements.

His research and teaching interests include analysis and synthesis of robust and adaptive control systems for control objects and processes with uncertain parameters.

E-mail: saga@tpu.ru

ORCID iD: 0000-0002-7156-2807

Tatiana Ezangina received the Ph. D. degree in system analysis, control and data processing from Tomsk Polytechnic University, Russia in 2016. She is presently a junior researcher of Telecommunications, Electronics and Underwater Geology Laboratory, National Research Tomsk Polytechnic University, Russia. She was repeatedly awarded by the Government of Russian Federation, Ministry of Education and Science of Russian Federation, Tomsk Polytechnic University and other institutions for her scientific achievements.

Her research interests include robust and adaptive control system analysis and synthesis, tethered underwater vehicles development and software development.

E-mail: eza-tanya@yandex.ru

ORCID iD: 0000-0002-4948-5972

Ivan Khozhaev received the B. Sc. and M. Sc. degrees (honors) in control systems engineering from the Tomsk Polytechnic University, Russia in 2014 and 2016, accordingly. He is presently a Ph. D. student at the Division for Automation and Robotics, the School of Computer Science and Robotics, National Research Tomsk Polytechnic University, Russia.

His research interests include robust and adaptive control systems synthesis and analysis, unmanned underwater vehicles development and computational fluid dynamics.

E-mail: khozhaev.i@gmail.ru (Corresponding author)

ORCID iD: 0000-0002-8874-0200

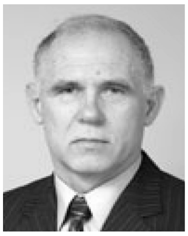

Viktor Kazmin received the Ph. D. degree in control systems engineering from the Tomsk Polytechnic University, Russia in 1996. He is presently an associated professor of the Division for Automation and Robotics at the School of Computer Science and Robotics, National Research Tomsk Polytechnic University, Russia. He was repeatedly awarded by Tomsk Polytechnic University for his educational achievements.

His research and teaching interests include analysis and synthesis of feedback control systems for internal combustion engines, fundamentals of control theory and automated control.

E-mail: kvp@tpu.ru